Quest Journals
Journal of Architecture and Civil Engineering
Volume1 ~ Issue 1 (2013) pp: 01-14
ISSN(Online) : 2321-8193
www.questjournals.org

Research Paper

Coupled Fluid-Thermal-Mechanical Analyses of a Deep Underground Coal Gasification Cavity

Hossein Akbarzadeh[1], Richard J. Chalaturnyk[1]

[1]*Department of Civil & Environmental Engineering, University of Alberta, Edmonton, Alberta, Canada*

Received 03 November, 2013; **A**ccepted 30 November, 2013

ABSTRACT: *Although underground coal gasification (UCG) has been tested in many countries as an environmentally friendly technique for gasification of deep un-mineable coal seams in situ, there are geomechanical risks during and post operation of UCG. It is a thermal-hydro-chemical-mechanical process. Evolution of the cavity along with high temperature may result in fracturing and collapsing of the formation adjacent to the gasification chamber as well as groundwater contamination. This paper presents results of a series of 3D coupled fluid-thermal-mechanical simulations of an example deep UCG site to evolution of a cubic cavity. The numerical simulation model included caprock on top, a layer of coal in the middle including a cubic cavity under syngas pressure and temperature, and underburden rock. Five scenarios were studied in order to investigate impacts of different operational conditions and material properties on the geomechanical response of the strata to UCG activity. This study revealed that evolution of the cavity containing high temperature syngas resulted in large volumetric strain and change in pore pressure as well as increase in mean effective stress and mechanical failure of the strata around the cavity. Impacts of running UCG plant under different operational pressures as well as using temperature-dependent elastic modulus and permeability for coal on the geomechanical response of the strata was also investigated.*

Keywords: Cavity, Coupled Fluid-Thermal-Mechanical, Geomechanics, UCG, Underground Coal Gasification

I. INTRODUCTION

I.1. Advantages of UCG

The 2010 Survey of Energy Resources estimated world coal reserves about 860 billion tonnes. Since 2000, global coal consumption has grown faster than any other fuel – at 4.9% per year- and is expected to rise by over 60% by 2030 [1] which asks for more coal extraction. There are greater resources deep underground that can be a supplement to the proved reserves but, based on current technology, are not economic to be mined. Underground coal gasification (UCG) has been identified as an environmentally friendly technique that can address the extra demands for coal consumption with the gasification of deep un-mineable coal seams, but with substantially less capital expenses and a smaller CO_2 footprint compared to the equivalent conventional surface gasifiers[2].

I.2. UCG Risks

Although UCG has been tested and trialed in many countries across the world [2], because of the nature of the process, which is a coupled thermal-hydro-chemical-mechanical process, there are always geomechanical risks in a UCG operation. Evolution of the cavity along with high temperature well over 1000 degrees Celsius as well as change in pore fluid pressure may result in fracturing and collapsing of the formation adjacent to the gasification chamber. Subsidence of the ground surface in shallow UCG and contamination of ground water are the other risks associated with the UCG projects.

*Corresponding Author: Hossein Akbarzadeh

Department of Civil & Environmental Engineering, University of Alberta, Edmonton, Alberta, Canada

I.3. Previous Studies of UCG

In order to optimize the UCG process and mitigate risks during and after gasification, extensive laboratory, analytical, and numerical studies as well as field monitoring have been done. Laboratory studies of mechanical, thermal and hydraulic properties of coals from different basins were performed [3, 4, and 5]. A few coal gasification experimental set ups were utilized under laboratory conditions [6, 7,8,and9].

Numerous analytical models were also developed for cavity growth prediction mainly based on the chemical process of combustion [10,11,and 12]. Rate of syngas production, its composition and temperature as well as change in porosity and permeability of the coal seam due to gasification (which leads to formation of a cavity) has been the focus of numerical simulations [6, 8,13,14,15,and 16].

A few field monitoring results of UCG trial sites were also published [17 and18]. Recently, the world's deepest ever UCG pilot test was successfully conducted at depth of 1400 m in Swan Hills, Alberta, Canada [19]. Geomechanical module of a UCG project has two important aspects. First, geomechanical response of the strata to the coal gasification process can determine the level of risk or safety of the UCG project site. Second, failure, cracking, deformation and, in general, geomechanical changes in coal and rock layers around the cavity will influence the chemical process of coal gasification by changing the flow properties e.g. porosity and permeability. Geomechanical simulations can provide the opportunity to predict the response of the coal seam and the surrounding formation to coal gasification and allows investigating caprock and bedrock integrity at different timesteps and under different operational conditions. To date, limited geomechanical simulations of UCG process have been published. Advani et al. [20 and 21] analyzed plane strain linear thermoelastic finite element models with an elliptical cavity within which high temperature and pressure was applied to investigate the tangential stress changes around the cavity. Tan et al. [22] performed plane strain finite element simulation of a UCG cavity with the aid of ANSYS software. To represent UCG process, high temperature was applied to the boundaries of the cavity, but no considerations was done for groundwater or syngas pressure. They used temperature dependent thermal and mechanical properties for coal and rocks and conducted coupled thermal-mechanical analysis in order to study changes in stress. Vorobiev et al. [23] performed two-dimensional finite element modeling of a disc-shaped reservoir. To simulate UCG activities, they did element removal and observed stress redistribution and surface subsidence. The pressure and temperature in the cavity was set to zero and elastic material was assumed. Three-dimensional modeling of an UCG cavity was done by Morris et al. [24] using LDEC (Livermore Distinct Element Code) by assuming an initial, instantaneous cavity and then predicting and removing the portions of the coal mass rendered unstable by the excavation, in the presence of gravity and an in situ stress field but without considerations for gasification temperature and groundwater or syngas pressure. They also examined influence of coal cleat orientation and persistence on the cavity evolution. Lawrence Livermore National Laboratory recently developed a new integrated 3D UCG simulator which is capable of both gasification and geomechanical simulations of UCG [25] however this package is not commercially available to the public.

I.4. Scope and Objectives of this Research

Published geomechanical modeling of UCG did not consider syngas pressure and temperature, and mechanical impacts together hence, a set of 3D fluid-thermal-mechanical analyses may represent the field behavior more realistically.The main objective of this study was to investigate the response of an example UCG site in a high in-situ stress condition (deep UCG) to evolution of a cubic cavity along with syngas pressure and temperature being applied to the cavity. A series of 3D fluid-thermal-mechanical simulations were conducted for five scenarios having different operational conditions and material properties.

II. DESCRIPTION OF THE SIMULATION MODEL

In this study, FLAC3D 4.00 of ITASCA was used. FLAC3D is a three-dimensional explicit finite-difference program for modeling advanced geotechnical/geomechanical analyses of soil and rock media to calculate stress and deformation, fluid flow, and heat conduction and convection using several built-in material models [26]. The geometry of the simulation model, initial configuration and material properties are explained in the following sub-sections.

*Corresponding Author: Hossein Akbarzadeh

Department of Civil & Environmental Engineering, University of Alberta, Edmonton, Alberta, Canada

II.1. Geometry

The model studied in this paper included three geological units; a coal seam overlaid with a layer of caprock on top and underlain with underburden rock layer. Thicknesses of these layers from top to the bottom are 247, 6, and 247 m, respectively. The model dimensions in both X and Y directions are 2000 m. A cubic cavity with the size of $6 \times 6 \times 6$ m, which extended to the entire thickness of the coal seam, was considered. Fig. 1 shows one quarter of the model that was constructed in FLAC3D software in order to reduce the simulation runtime. As shown in Fig. 1, a finer mesh was adopted around the cavity to capture geomechanical changes more accurately however the mesh became coarser farther away from the cavity. The total number of grid points and zones were 3751 and 2970, respectively. Also shown in Fig. 1 are the locations of four monitoring points on the perimeter of the cavity. Point A is the top center, B is the bottom center, C is the center point along the X-axis, and point D is the center point along the Y-axis of the cavity.

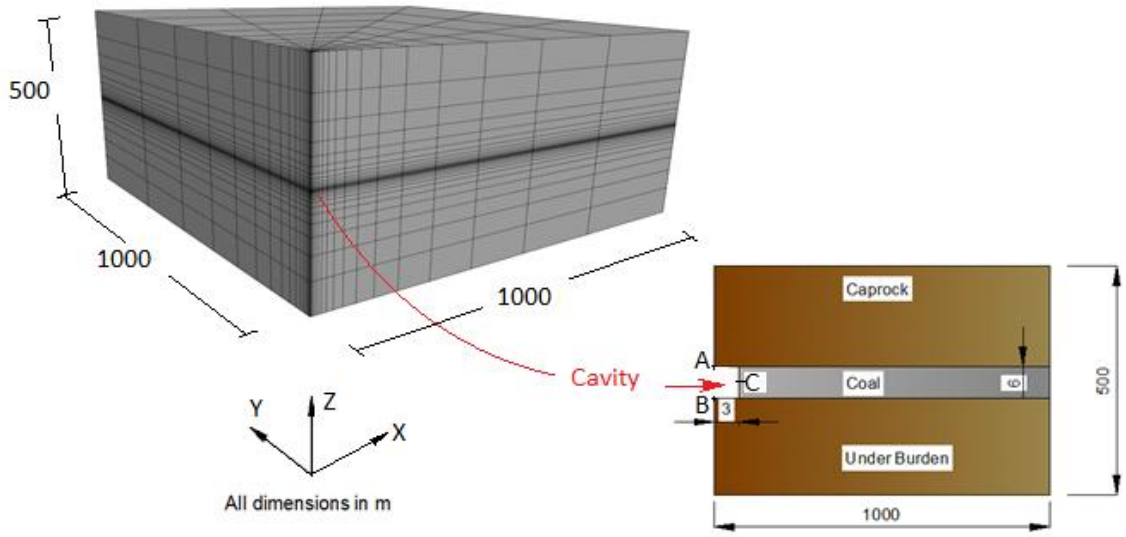

Figure1: 3D finite difference mesh and the cavity used in the analyses

II.2. Initial Configurations and Material Properties

In the geomechanical simulations, the bottom of the model was fixed, sides were selected as rollers and top of the caprock was assigned free boundary. High initial in-situ stress corresponding to a depth of 1400 m was assigned to the model such that total vertical stress at the middle of the coal seam was $\sigma_x = \sigma_y = \sigma_z = 31\ MPa$. Stress ratios for X and Y directions was chosen as unity. The initial hydrostatic pore pressure was assigned to the model such that pore pressure at the middle of the coal seam was 11.5 MPa. Initial temperature for the formation was set equal to 60^{o}C.

A set of input material properties was selected for the fluid-thermal-mechanical analyses as summarized in Table 1. The rock layers were considered mechanically stronger but 10 times less porous than the coal however thermal conductivity or the rock materials was greater than the coal. It should be noted that the permeability used in FLAC3D is actually a mobility coefficient and defined as the ratio of the intrinsic permeability to the fluid dynamic viscosity. The equivalent permeability in *millidarcy*(mD) unit for the coal and rock are 1 and 0.1, respectively. All strata were assumed homogeneous and isotropic, and Mohr-Coulomb elastic perfectly plastic model was selected for mechanical analyses for both coal and rock layers using the corresponding parameters shown in Table 1. Isotropic fluid flow and isotropic thermal flow was also considered for all layers.

After initializing the initial in-situ stress condition, the cavity was excavated. To simulated UCG process, average temperature of 500 ºC was applied to the cavity boundaries. Syngas pressure in the range of 10 to 13 MPa was considered as a constant fluid pressure at the cavity boundaries. The reservoir pressure in this simulation is 11.5 MPa for which the steam saturation temperature is about 320 ^{o}C[27]. Blocks of coal and rock in the vicinity of the cavity may experience temperatures above the steam saturation temperature, i.e. pore water

*Corresponding Author: Hossein Akbarzadeh

Department of Civil & Environmental Engineering, University of Alberta, Edmonton, Alberta, Canada

will change phase from liquid water to steam. In a similar temperature and pressure condition in a real UCG site, there is a mix of other gases such as CH_4, CO, CO_2, and H_2, but this simulation assumed single-phase Darcy fluid flow. Any interactions between syngas, steam and water as well as chemical reaction between syngas and coal was not included.

Table 1: Geomechanical, thermal, and fluid properties of the coal and rock used in this study

Property	Coal	Rock
Elastic Modulus, E (MPa)	5000	30000
Poisson's Ratio, υ	0.3	0.3
Friction Angle, $\phi(°)$	40	60
Cohesion, C (MPa)	10	35
Density (Kg/m^3)	1200	2500
Porosity (%)	0.0866	0.05
Permeability $\times 10^{-13}$ ($m^2/Pa.sec$)	9.81	0.981
Thermal Conductivity, k (W/mo_C)	0.3	2.5
Specific Heat, C_v (J/Kgo_C)	1400	1100
Coefficient of Linear Thermal Expansion, $\alpha_t \times 10^{-6}(1/℃)$	9	15
Fluid Bulk Modulus (GPa)	1.5	1.5
Fluid Density (Kg/m^3)	1000	1000
Fluid Volumetric Thermal Expansion Coefficient, $3\alpha_f$ ($1/℃$) (@ P= 11.5 MPa, t= 100 ℃)	0.734×10^{-3}	0.734×10^{-3}
Matrix Volumetric Thermal Expansion Coefficient, β ($1/℃$) (@ P= 11.5 MPa, t= 100 ℃)	88.3×10^{-6}	79.5×10^{-6}

II.3. Coupled Fluid-Thermal-Mechanical Analyses

UCG operation imposes significant geomechanical changes to the strata. The cavity evolution introduces mechanical deformation which in turn influences fluid pressure. Syngas extraction, while running the UCG plant at a pressure different from initial reservoir fluid pressure, causes mechanical deformation and alters the in situ stress condition. These are in compliance with the Biot's three-dimensional theory of poroelasticity which states that a change in stress produces a change in fluid pressure or fluid volume in a porous medium likewise a change in fluid pressure or volume yields a change in the volume of a porous medium [28]. High temperature of coal gasification causes thermal stress and deformation as well as thermally-induced pore pressure. All the aforementioned geomechanical perturbations happen simultaneously which ask for a coupled fluid-thermal-mechanical analysis.

The fluid flow capability of FLAC3D is applicable to any problem involving single-phase Darcy flow of any type of fluid in a porous medium. It requires information regarding the variables pore pressure, saturation and the three components of the specific discharge vector. The thermal module of FLAC3D incorporates both conduction and advection models. Only conduction was included in the simulation for this study. The variables involved in heat conduction in FLAC3D are the temperature and the three components of the heat flux. Any of the fluid, thermal, mechanical modules can be run independently or coupled to the others.

The formulation of coupled fluid-mechanical processes in FLAC3D is based on the Biot's theory of poroelasticity. The variables in the coupled fluid-thermal-mechanical module are related through the Darcy's law for fluid transport, balance laws (fluid mass balance equation, thermal energy balance equation, momentum balance equation), and a constitutive law relating changes in pore pressure to saturation, volumetric strains, and temperature [26]. The material properties used in the coupled analyses of this study are provided in Table 1.

The fluid-thermal-mechanical constitutive law in FLAC3D has the general form of Equation 1. This Equation allows calculation of change in pore pressure due to temperature change and deformation of the saturated matrix.

*Corresponding Author: Hossein Akbarzadeh

Department of Civil & Environmental Engineering, University of Alberta, Edmonton, Alberta, Canada

$$\frac{\partial P}{\partial t} = M\left(\frac{\partial \zeta}{\partial t} - \alpha\frac{\partial \epsilon}{\partial t} + \beta\frac{\partial T}{\partial t}\right) \quad (1)$$

whereζ is the variation of fluid content, M is the Biot modulus, α is the Biot coefficient (equal to 1 for incompressible solid grains), ϵ is the volumetric strain, and β is the undrained volumetric thermal expansion. The Biot modulus is related to the fluid bulk modulus, K_f, and porosity, *n*, through Equation 2:

$$M = \frac{K_f}{n} \quad (2)$$

For an ideal porous material, β is related to the volumetric thermal expansion coefficients for the grains, $3\alpha_t$, and the fluid, $3\alpha_f$, through Equation 3:

$$\beta = 3\left[\alpha_t(\alpha - n) + \alpha_f n\right] \quad (3)$$

Equation 1 gives some insights about the contributions of the three constituents on pore pressure change; namely fluid content in the pore space, deformation of the matrix, and temperature of the matrix. Based on Equation 1, adding more fluid to the pore space will increase the pore pressure likewise, increase in temperature will raise the pore pressure. Volumetric strain has a reverse effect on pore pressure. If the matrix expands, pore pressure will drop and vice versa.

To perform a coupled fluid-thermal-mechanical simulation of a UCG cavity, the following steps were taken. The initial configuration was run for mechanical equilibrium, a cavity was created, and then a series of thermal, mechanical and fluid steps were followed until the intended simulation time was met. Each step includes one thermal loop, followed by enough mechanical steps (to maintain quasi-static equilibrium) and sufficient flow loops which was again followed by enough mechanical steps after every flow step. It should be noted that fluid timestep for this simulations was orders of magnitude smaller than thermal timestep hence, a mechanism was coded in FLAC3D in order to synchronize the fluid and thermal times by performing enough fluid loop per each thermal loop.

II.4. Description of the Five Scenarios Studied

The numerical simulations were performed on five different scenarios to investigate impacts of different operational pressure and material properties on the geomechanical response of the cavity. The cavity temperature for all scenarios was 500 ℃. Information regarding the five scenarios is presented below which is summarized in Table 2.

Table 2: Summary of the five numerical simulation scenarios

Scenario	Cavity Temperature (℃)	Syngas Pressure (MPa)	Deviation in Material Properties from Table 1
1	**500**	**11.5**	**-**
2	**500**	**10**	**-**
3	**500**	**10**	**Temperature-dependent elastic modulus for coal seam (as in Fig. 2)**
4	**500**	**10**	**Temperature-dependent permeability for coal seam (as in Fig. 3)**
5	**500**	**13**	**-**

II.4.1. Scenario 1

This scenario used constant material properties as in Table 1. The syngas pressure for scenario 1 was selected as 11.5 MPa which is equal to the initial reservoir pressure at the middle of the coal seam. With that being said any changes in pore pressure after running the model is supposed to be due to the thermally-induced

pore pressure caused by the elevated temperature and/or mechanically-induced pore pressure because of the perturbation caused by the cavity evolution.

II.4.2. Scenario 2

This scenario was the same as scenario 1, except syngas pressure (which was 10 MPa) was below the initial pore pressure in the middle of the coal seam (which was 11.5 MPa). UCG practitioners prefer to operate the plant below the initial reservoir pressure to prevent syngas diffusion to adjacent strata and instead having water influx to the gasification chamber. This will reduce contaminant transport to ground water.

II.4.3. Scenario 3

This scenario had similar specifications to scenario 1; except it used 10 MPa for syngas pressure and elastic modulus of the coal was assumed to be temperature-dependent. Like any mechanical properties of coal, elastic modulus of coal changes at elevated temperature. Change in elastic modulus of coal specimens from Hanna Basin coal was studied by Glass, 1984 [4]. He carried out triaxial experiments up to 250 ºC and uniaxial tests conducted in air at 350 ºC and 450 ºC, perpendicular and parallel to the bedding plane. Normalized elastic moduli of Hanna Basin are plotted versus temperature in Fig. 2. It can be seen in Fig. 2 that there was an initial gain in elastic modulus at temperature of 80 ºC in direction parallel to bedding plane. The normalized elastic modulus curves approached the abscissa at temperature about 350 ºC however in direction normal to bedding plane, continuous decline of elastic modulus occurred during heating. The solid step-wise function in Fig. 2 is the one adopted for this simulation. Elastic moduli of coal blocks were calculated as the multiplication of the initial elastic modulus of the blocks (as in Table 1) and the normalized values at the corresponding temperatures from the solid step-wise function in Fig. 2.

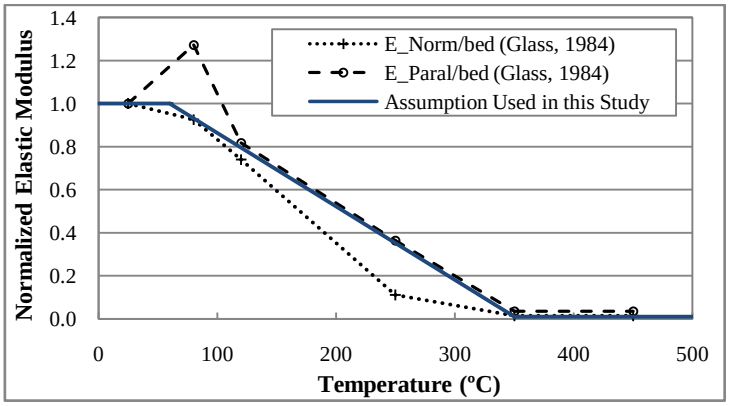

Figure 2: Normalized elastic modulus of Hanna Basin coal versus temperature normal and parallel to bedding plane [4] and the assumed function used for scenario 3

II.4.4. Scenario 4

For this scenario syngas pressure was 10 MPa and temperature-dependent permeability was used for coal. As a coal specimen is heated, its permeability increases. Thermal deformation and microcrack generation as well as release of volatile matters during heating of coal result in change in pore volume and permeability of coal matrix. Thorsness et al., 1978 [29] investigated change in permeability of Wyodak coal specimens during drying and pyrolysis. The ratios of permeability of Wyodak coal at elevated temperatures to the corresponding values at ambient temperature (which was 20 ºC) are plotted against temperature in Fig. 3. Although the data points show an exponential trend but a line could be fitted to the initial linear part of the data points. A line was selected such that it reasonably fits the data points for temperature in the range of 60 to 500 ºC. The assumed line predicts normalized permeability equal to 1 and 125 at temperature of 60 and 500 ºC, respectively.Permeability of coal blocks in the heated area around the cavity was calculated as the multiplication of the initial permeability of the blocks (as in Table 1) and the normalized values at the corresponding temperatures.

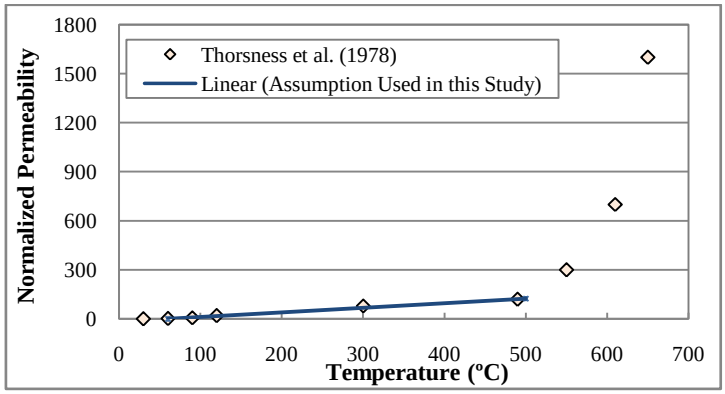

Figure 3: Normalized permeability of Wyodak coal versus temperature [29]and the assumed function used for scenario 4

II.4.5. Scenario 5

In this scenario, everything was identical to scenario 1, except syngas pressure that was selected equal to 13 MPa which was above the initial reservoir pressure. The intention for this scenario was to get some insight about how the geomechanical response would change if the UCG plan loses operation and exceeds the reservoir pressure. It is worth-mentioning that the environmental influence of such a loss was not in the scope of this study.

III. RESULTS AND DISCUSSIONS

This section provides some geomechanical responses for all scenarios (Fig.s 4 to 9) and discussions on the results. The geomechanical responses include changes in temperature and pore pressure, mean effective stress and volumetric strain in the middle of the coal seam as well as base of the caprock. It should be noted that the coordinates for Fig.s 5 to 9 were set on the center of the cavity. Magnitudes of displacements of four monitoring points on the boundary of the cavity (points A, B, C, and D in Fig. 1) are shown in Fig. 10.

III.1. Results of Scenario 1

Fig. 4 includes some of the observed changes in the strata after 182 days. Fig. 4.a shows temperature contour. As it can be seen in this figure, temperature front extended more into the rock layers than in the coal seam which is because of this fact that thermal conductivity of the rock was chosen greater than the coal seam (Table 1). The displacement contour is presented in Fig. 4.b which shows that larger deformation happened around the cavity. This is also in compliance with the volumetric strain contour shown in Fig. 4.c. One important issue in underground activities such as UCG is maintaining caprock and bedrock integrity. Investigating development of plastic zone around the UCG reactor and potential failure of the caprock, bedrock and the adjacent coal material is of significant importance as the materials in the plastic zone may undergo large deformation which can lead to failure or at least increase in porosity and permeability. Combination of thermal stress induced by high temperature of coal gasification and mechanical perturbation caused by the cavity evolution were the reasons for strain localization and consequently forming a plastic zone around the perimeter of the cavity which is seen in Fig. 4.d.

Fig. 5 shows plots of changes in temperature and pore pressure, mean effective stress and volumetric strain in the middle of the coal seam as well as base of the caprock. Fig. 5.a shows distribution of changes in temperature and pore pressure versus distance on the middle of the coal seam at different times; 1, 10, 30, and 182 days. By time, temperature front moved farther from the cavity boundary which resulted in decline of pore pressure. Similar behavior was observed in base of the caprock (Fig. 5.b). Mean effective stress and volumetric strain in coal and caprock are shown in Fig. 5.c and d, respectively. Initial mean effective stress in the middle of the coal seam and base of the caprock was about 20 MPa which increased significantly due to UCG activity such that after 182 days, maximum mean effective stress in in the middle of the coal seam and base of the caprock was 64.6 and 162.0 MPa, respectively. The corresponding values for volumetric strain were 0.022 and 0.030, respectively.

*Corresponding Author: Hossein Akbarzadeh

Department of Civil & Environmental Engineering, University of Alberta, Edmonton, Alberta, Canada

Based on Fig. 5, it can be concluded that due to the cavity evolution and high temperature of syngas, large volumetric strain happened around the cavity. The amount of observed volumetric strain in base of the caprock was greater than the middle of the coal seam. Because of the large deformation of the strata around the cavity, pore pressure in the coal and rock declined. Similar trends of pore pressure responses were observed in the coal and caprock. At later times, either syngas diffused or water moved from farther points to the pore pressure decline area which compensated pore pressure drops (Fig. 5.a and b).

Besides the large deformation of the strata around the cavity, mean effective stress in the coal and base of the cap rock also increased. Base of the caprock experienced larger mean effective stress than the middle of the coal seam. The maximum mean effective stress in the base of the cap rock occurred close to the top corner of the cavity. Moreover, it was found out that the UCG influence on pore pressure profiles extended to a larger distance from the cavity (a few hundred meters) that its influence on temperature, mean effective stress, and volumetric strain profiles. This fact can be seen in Fig. 5.a and b through Fig. 9.a and b.

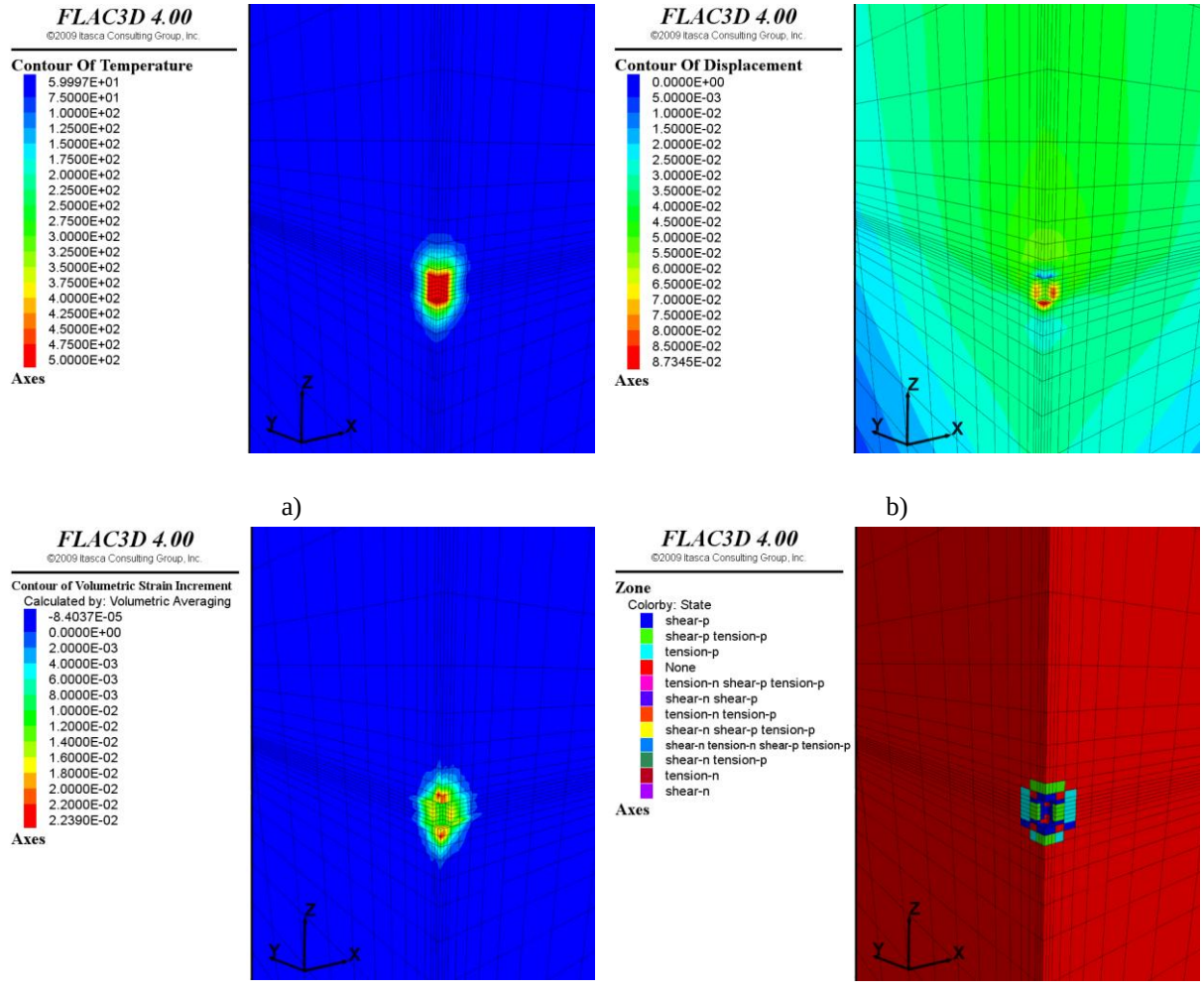

Figure 4: Contours from scenario 1 after 182 days: a) temperature, b) displacement, c)volumetric strain, and d) plastic zone around the cavity

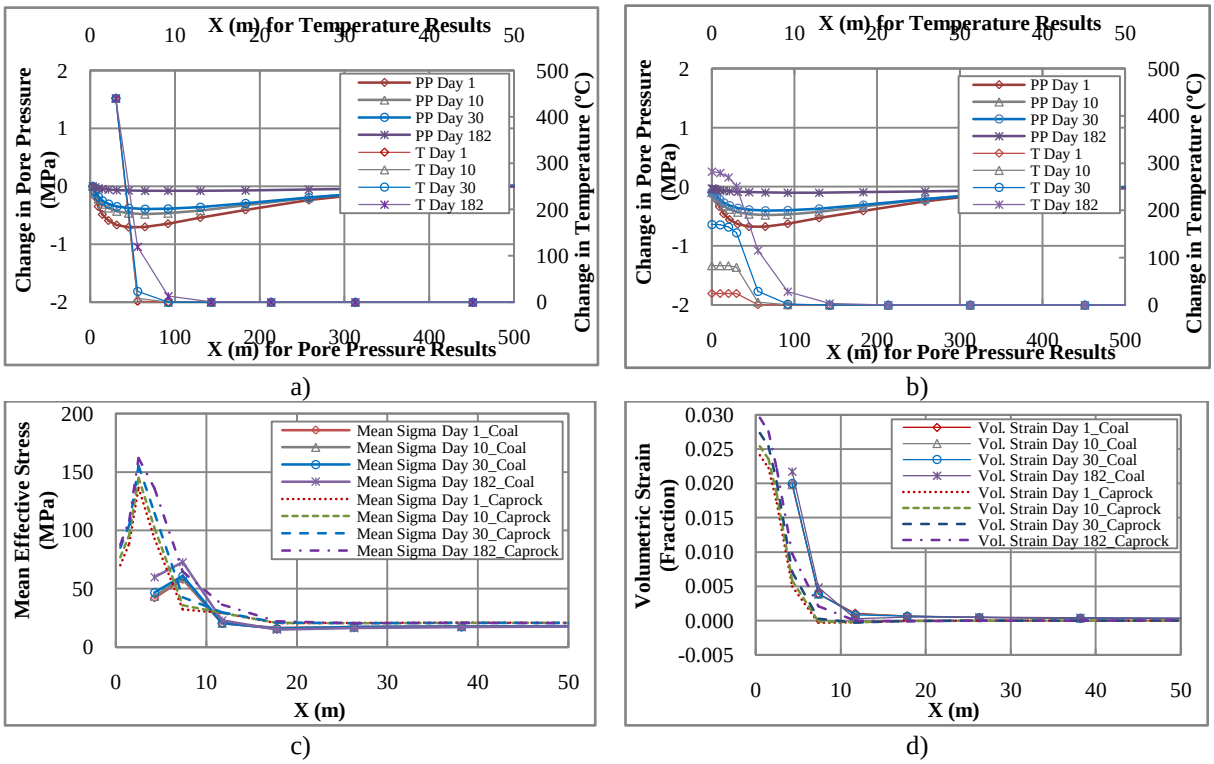

Figure5: Results from scenario 1: a) change in pore pressure and temperature along middle of the coal seam, b) change in pore pressure and temperature along base of the caprock, c) mean effective stress along middle of the coal seam and base of the caprock, and d) volumetric strain along middle of the coal seam and base of the caprock

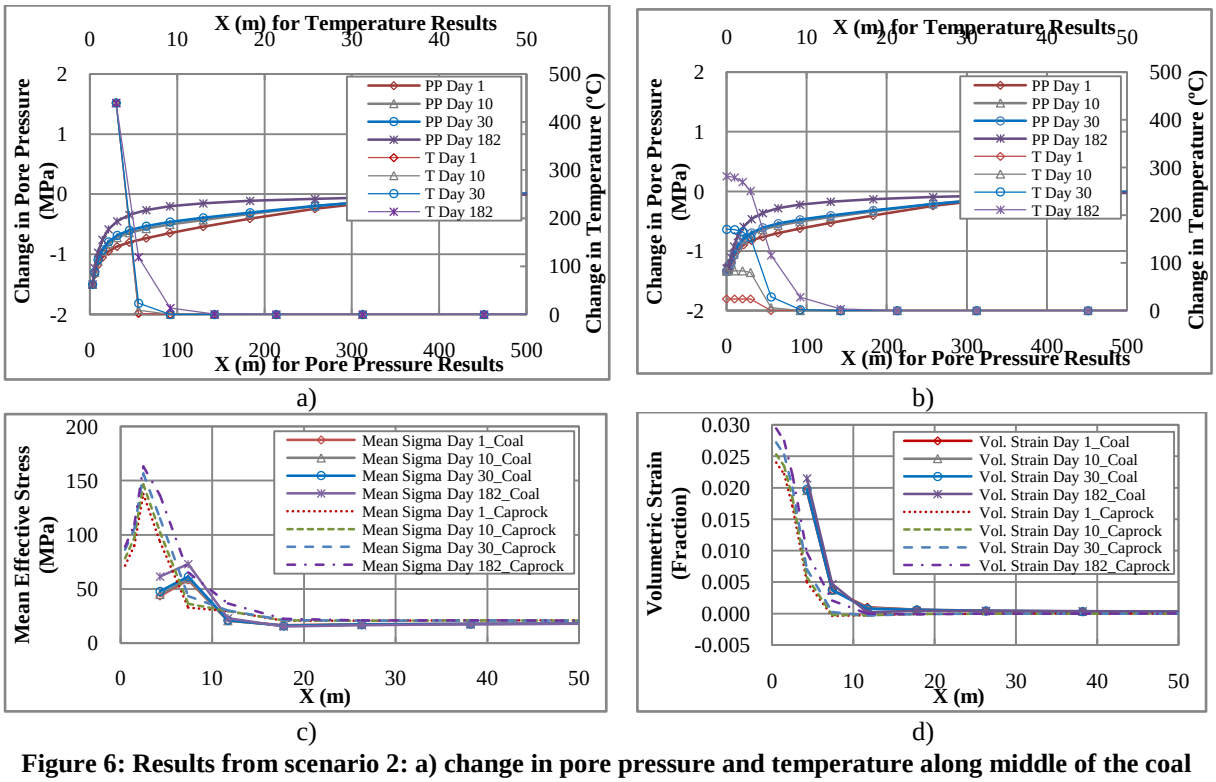

Figure 6: Results from scenario 2: a) change in pore pressure and temperature along middle of the coal seam, b) change in pore pressure and temperature along base of the caprock, c) mean effective stress along middle of the coal seam and base of the caprock, and d) volumetric strain along middle of the coal seam and base of the caprock

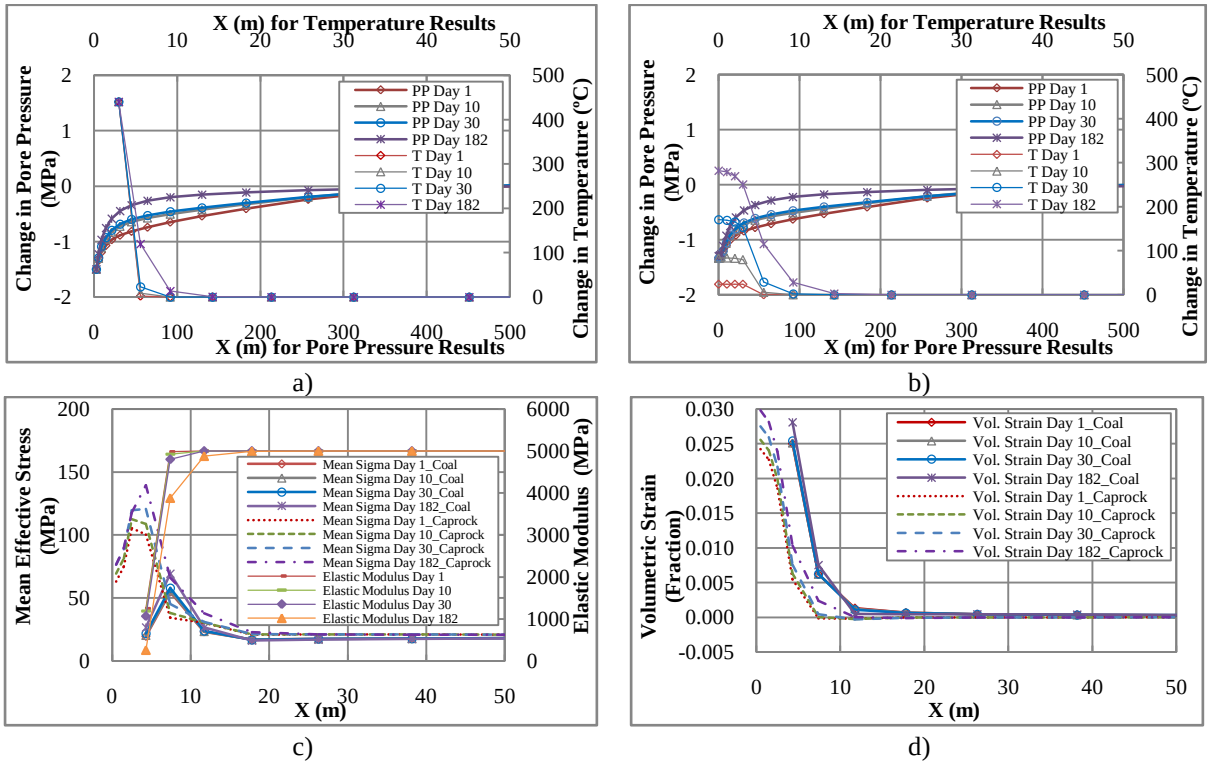

Figure 7: Results from scenario 3: a) change in pore pressure and temperature along middle of the coal seam, b) change in pore pressure and temperature along base of the caprock, c) mean effective stress and elastic modulus along middle of the coal seam as well as mean effective stress along base of the caprock, and d) volumetric strain along middle of the coal seam and base of the caprock

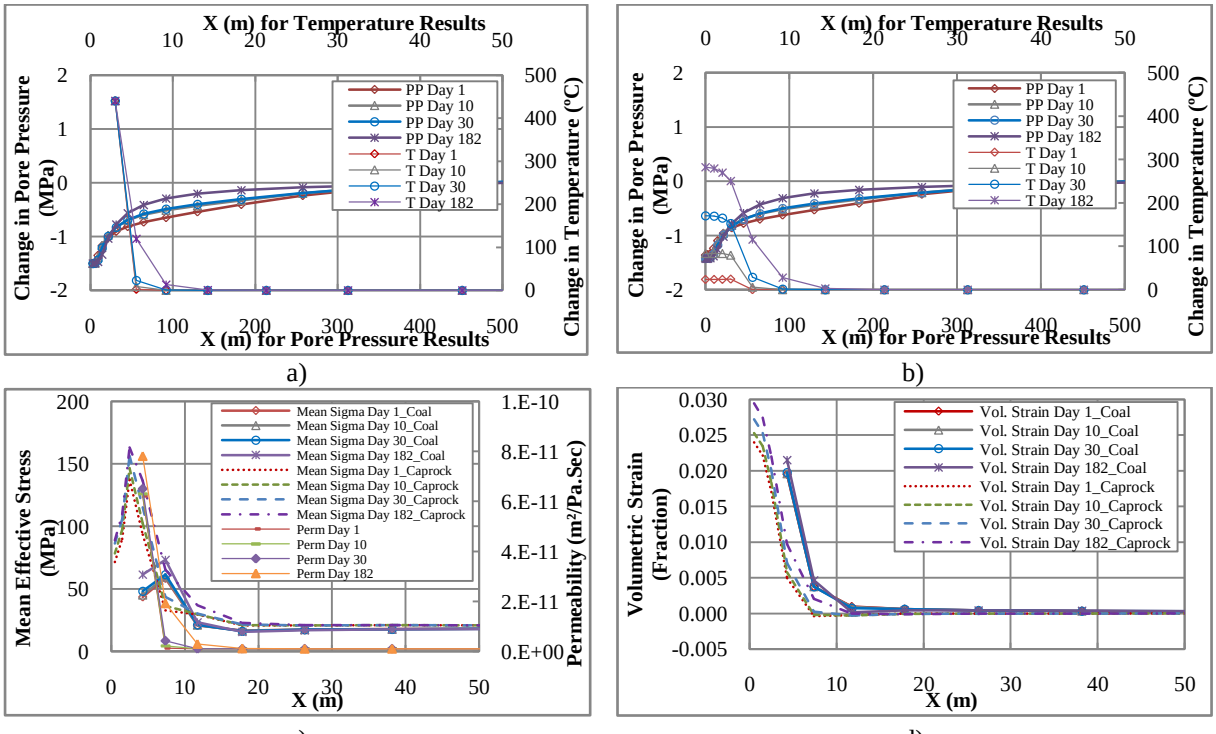

Figure 8: Results from scenario 4: a) change in pore pressure and temperature along middle of the coal seam, b) change in pore pressure and temperature along base of the caprock, c) mean effective stress and permeability along middle of the coal seam as well as mean effective stress along base of the caprock, and d) volumetric strain along middle of the coal seam and base of the caprock

*Corresponding Author: Hossein Akbarzadeh

Department of Civil & Environmental Engineering, University of Alberta, Edmonton, Alberta, Canada

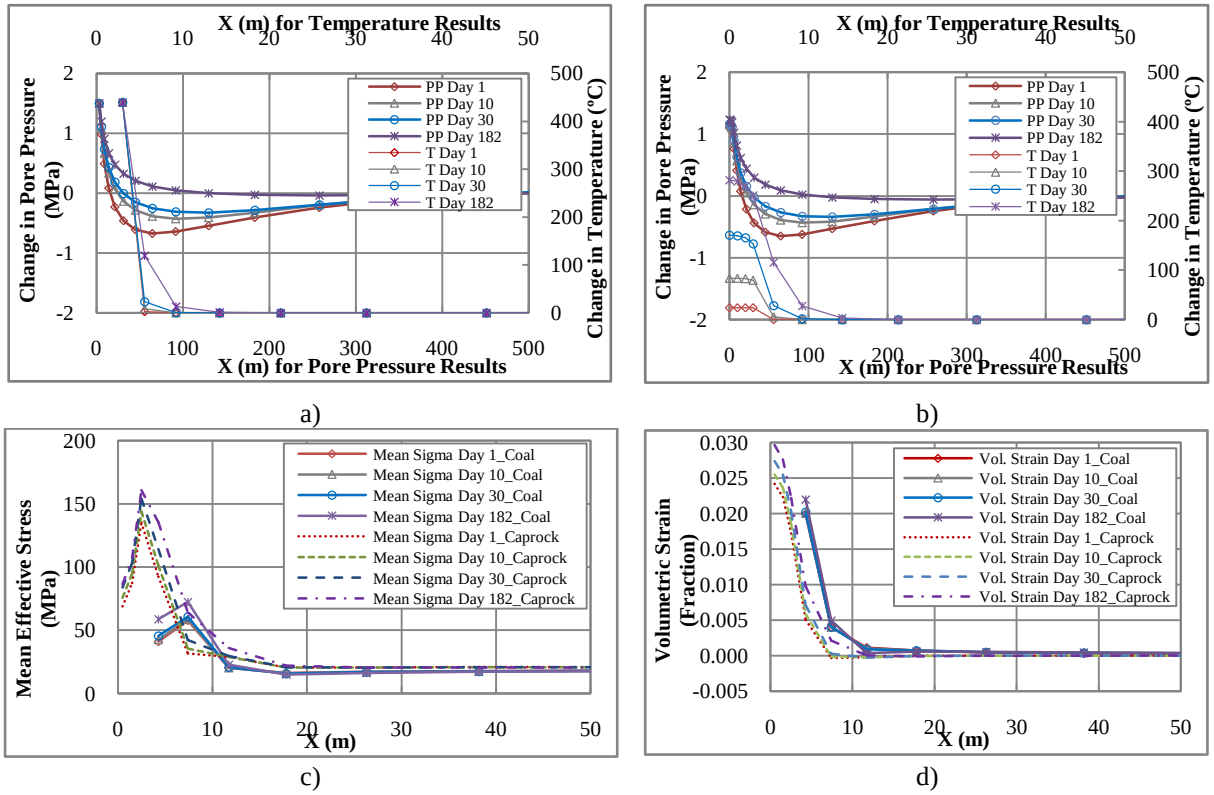

Figure 9: Results from scenario 5: a) change in pore pressure and temperature along middle of the coal seam, b) change in pore pressure and temperature along base of the caprock, c) mean effective stress along middle of the coal seam and base of the caprock, and d) volumetric strain along middle of the coal seam and base of the caprock

III.2. Impacts of Syngas Pressure on the GeomechanicalResponse

For scenarios 1, 2 and 5 the value of syngas pressure was selected equal to, less than, and greater than initial pore pressure. As it can be seen in sub-sections a and b of Fig.s 5, 6, and 9, base of the caprock and middle of the coal seam exhibited similar pore pressure responses despite the fact that permeability of the rock layers was one order of magnitude smaller than the coal seam. No matter what the syngas pressure was, in all cases, in early ages, pore pressure dropped in the vicinity of the cavity and then increased by time. In scenario 1 which the syngas pressure was chosen equal to the initial pore pressure, after 182 days pore pressure returned back to the initial pore pressure (Fig. 5.a and b). In scenario 2, the formation maintained the pressure difference between syngas and initial reservoir pressure (Fig. 6.a and b). Although for scenario 5 the syngas pressure was selected above the initial reservoir pressure, in the early ages, pore pressure a few meters away from the cavity, pore pressure dropped. Later, pore pressure gained value and experienced some rise.

Change in syngas pressure through scenarios 1, 2, and 5 did not show significant impacts on volumetric strain and mean effective stress in the coal and caprock. This simulation study only considered thermal conduction however thermal convection was not included hence, change in syngas pressure did not create any influence on temperature plots.

III.3. Impacts of Temperature-Dependent Coal Elastic Modulus on the Geomechanical Response

Decline of elastic modulus of coal as a function of temperature for different simulation times are shown in Fig. 7.c. In comparison to scenario 2, by considering temperature-dependent stiffness, coal became softer around the cavity which allowed more deformation and larger volumetric strain in the coal however smaller mean effective stress was observed just next to the cavity in both the coal seam and the caprock. This assumption did not result in any changes to the temperature plots.

III.4. Impacts of Temperature-Dependent Coal Permeability on the Geomechanical Response

By this assumption, coal permeability exhibited up to two orders of magnitude changes in the vicinity of the cavity where high temperature gradient existed (Fig. 8.c). The initial permeability of coal, just next to the cavity, was $9.81 \times 10^{-13} (m^2/Pa.sec)$ which increased to $7.82 \times 10^{-11} (m^2/Pa.sec)$ after 182 days. It was observed that because of the enhanced coal permeability around the cavity, compared to scenario 2, pore pressure in coal and base of the cap rock rapidly reached the steady state condition. No changes were seen in temperature front as thermal convection was not included in these simulations. This assumption did not create any noticeable changes to volumetric strain and mean effective stress plots in the coal and rock.

III.5. Displacements of the Monitoring Points through Scenarios 1 to 5

Displacements of the four monitoring points are plotted in Fig. 10. In all scenarios, points A to D moved towards to the center of the cavity which indicates that the strata deformed towards the cavity. Each monitoring point had almost the same displacement throughout the scenarios except scenario 3 which used temperature dependent elastic modulus for coal. Since in scenario 3 coal stiffness declined in the vicinity of the cavity as a function of temperature, all monitoring points experienced larger displacements towards the center of the cavity. Displacements of points A, B, C, and D in scenario 3 were -0.021, 0.093, -0.142, and -0.128 m, respectively.

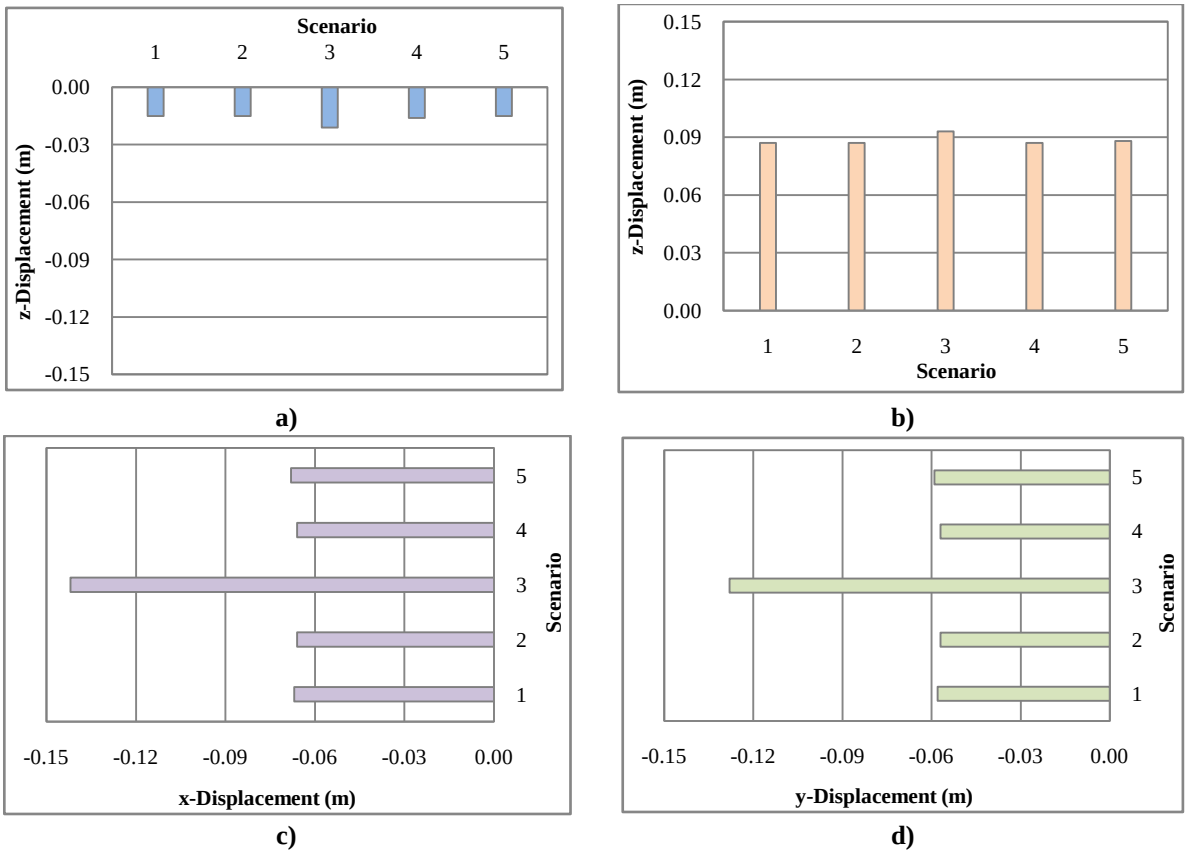

Figure 10: Displacements of the four monitoring points in different scenarios;a) point A, b) point B, c) point C, and d) point D

IV. SUMMARY AND CONCLUSIONS

To investigate geomechanical response an example deep UCG site to evolution of a cubic cavity along with syngas pressure and temperature, a series of 3D coupled fluid-thermal-mechanical simulations were conducted in FLAC3D software on a model for five scenarios having different operational conditions and material properties.The numerical simulation model included caprock on top, a layer of coal in the middle

including a fixed size cavity under syngas pressure and high temperature, and underburden rock. Based on the results obtained in this study, the following conclusions were drawn.

- Due to the cavity evolution and high temperature of syngas, large volumetric strain happened around the cavity.
- Base of the caprock experienced larger volumetric strain than the middle of the coal seam. Because of the large deformation of the strata around the cavity, pore pressure in the coal and rock dropped. At later times, pore pressure decline was compensated. Similar trends of pore pressure responses were observed in the coal and caprock.
- Mean effective stress in the coal and base of the cap rock increased. Base of the caprock experienced larger mean effective stress than the middle of the coal seam.
- For the three assumptions for syngas pressure, in early ages pore pressure dropped in the vicinity of the cavity and then increased by time.
- Change in syngas pressure did not show significant impacts on volumetric strain and mean effective stress in the coal and caprock.
- Using temperature-dependent elastic modulus for coal resulted in larger deformation and volumetric strain in the coal but smaller mean effective stress in both the coal seam and the caprock was observed.
- Using temperature-dependent permeability for coal helped pore pressure in the coal and base of the cap rock rapidly reached the steady state condition but no noticeable changes to volumetric strain and mean effective stress occurred.
- In all scenarios, the four monitoring points on the perimeter of the cavity moved towards the center of the cavity which indicates that the strata deformed towards the cavity. In scenario with temperature-dependent elastic modulus for coal, all monitoring points experienced larger displacements towards the center of the cavity.

ACKNOWLEDGEMENTS

The financial support for this study was provided by *the Canadian Centre for Clean Coal/Carbon and Mineral Processing Technologies*(C^5MPT).

REFERENCES

[1]. World Energy Council,2010 survey of energy resources(World Energy Council, London, UK, 2010).
[2]. E. Burton, J.Friedmann, R.Upadhye,Best Practices in Underground Coal Gasification(Draft, Lawrence Livermore National Laboratory, University of California, 2007).
[3]. M.K.Dabbous, A.A.Reznik, J.J. Taber,and P.F. Fulton, The permeability of coal to gas and water,SPE Journal 14(6),1974, 563-572.
[4]. R.E. Glass, The thermal and structural properties of a Hanna basin coal,Journal of Energy Resources Technology, ASME, 106,1984, 266-271.
[5]. Y. Zhao, F. Qu, Z. Wan, Y. Zhang, W. Liang, and Q. Meng,Experimental investigation on correlation between permeability variation and pore structure during coal pyrolysis,Transport in Porous Media,82(2), 2010, 401-412.
[6]. L. Yang,Study on the model experiment and numerical simulation for underground coal gasification,Fuel, 83, 2004, 573-584.
[7]. K.Kostur, J.Kacur,The monitoring and control of underground coal gasification in laboratory conditions, ActaMontanisticaSlovaca, 13,2008, 111-117.
[8]. S.Daggupati, R.N.Mandapati, S.M.Mahajani, A. Ganesh, D.K. Mathur, R.K. Sharma, and P. Aghalayam, Laboratory studies on combustion cavity growth in lignite coal blocks in the context of underground coal gasification, Energy, 35,2010, 2374-2386.
[9]. K. Stanczyk, K. Kapusta, M. Wiatowski, J. Swiadrowski, A. Smolinski, J. Rogut, and A. Kotyrba,Experimental simulation of hard coal underground gasification for hydrogen production,Fuel, 91, 2012, 40-50.
[10]. L.V.Fausett, An analysis of mathematical models of underground coal gasification,doctoraldiss., University of Wyoming, Laramie, Wyoming, USA, 1984.
[11]. K.S. Jung, Mathematical modeling of cavity growth during underground coal gasification. Doctoraldiss., University of Wyoming, Laramie, Wyoming, USA, 1987.
[12]. P.S.Sansgiry, A numerical technique to track the growth of cavities in underground coal gasification. Doctoraldiss., University of Wyoming, Laramie, Wyoming, USA, 1990.
[13]. T.A .Buscheck, Y.Hao, J.P. Morris, E.A. Burton, Thermal-hydrological sensitivity analysis of underground coal gasification,Proc. International Pittsburgh Coal Conference, Pittsburgh, PA, 20-23 September 2009
[14]. H.Nourozieh, M.Kariznovi, Z.Chen, and J. Abedi, Simulation study of underground coal gasification in Alberta reservoirs: geological structure and process modeling,Energy Fuels,24(6),2010, 3540-3550.

*Corresponding Author: Hossein Akbarzadeh

Department of Civil & Environmental Engineering, University of Alberta, Edmonton, Alberta, Canada

[15]. M.Seifi, Z. Chen, J.Abedi, Numerical simulation of underground coal gasification using the CRIP method,The Canadian Journal of Chemical Engineering, 89, 2011, 1528-1539.
[16]. A.SarrafShirazi,CFD simulation of underground coal gasification. Mastersdiss., University of Alberta, Edmonton, Alberta, Canada, 2012.
[17]. L.C.Bartel, S.G. Beard, L.W. Beckham, R.P. Reed, and R.W. Seavey,Instrumentation results from an in-situ coal gasification experiment,Proc. SPE Annual Fall Technical Conference and Exhibition, New Orleans, Louisiana, USA, 3-6 October 1976
[18]. X.Luo, Q. Tan, C.Luo, and Z. Wang, Microseismic monitoring of burn front in an underground coal gasification experiment,Proc.42nd U.S. Rock Mechanics Symposium (USRMS), San Francisco, CA, USA, June 29 - July 2 2008
[19]. Swan Hills Synfuels, Swan Hills in-situ coal gasification technology development; final outcomes report(Swan Hills Synfuels, Alberta, Canada, 2012).
[20]. S.H.Advani, Y.T.Lin, and L.Zane Shuck, Thermal and structural response evaluation for underground coal gasification,SPE Journal, 17(6),1977, 413-422.
[21]. S.H.Advani, L.Zane Shuck, Y.T.Lin, and H.Y. Chang, Thermomechanics simulations associated with underground coal gasification,Proc.17th U.S. Symposium on Rock Mechanics (USRMS), Snow Bird, UT, USA, 25-27 August 1976, 5 D4.1-5 D4.7.
[22]. Q. Tan, X.Luo, and S. Li, Numerical modeling of thermal stress in a layered rock mass,Proc. 42nd US Rock Mechanics Symposium and 2nd U.S.-Canada Rock Mechanics Symposium,San Francisco, CA, USA, June 29 - July 2 2008
[23]. O.Y.Vorobiev, J.P. Morris, T.H.Antoun, S.J. Friedmann, Geomechanical simulations related to UCG activities,Proc. International Pittsburgh Coal Conference, Pittsburgh, PA, USA, September 29 - October 2 2008
[24]. J.P. Morris, T.A.Buscheck, and Y.Hao, Coupled geomechanical simulations of UCG cavity evolution,Proc. International Pittsburgh Coal Conference, Pittsburgh, PA, USA, 20-23 September 2009
[25]. J.J.Nitao, D.W. Camp, T.A. Buscheck, J.A. White, G.C. Burton, J.L. Wagoner, and M. Chen, Progress on a new integrated 3-D UCG simulator and its initial application,Proc.International Pittsburgh Coal Conference, Pittsburgh, PA, USA, 12-15 September 2011
[26]. Itasca Consulting Group Inc,FLAC3D User's Guide, 2009 (Itasca Consulting Group Inc, Minneapolis, Minnesota, 2009).
[27]. American Society of Mechanical Engineers,ASME international steam tables for industrial use(Second Edition, American Society of Mechanical Engineers, New York, 2009).
[28]. M.A.Biot,General theory of three-dimensional consolidation,Journal of Applied Physics, 12(2), 1941, 155-164.
[29]. C.B.Thorsness, E.A.Grens, A.Sherwood,A one-dimensional model for in situ coal gasification(UCRL-52523, Lawrence Livermore, National Laboratory (LLNL) Report, Berkeley, California, 1978).